EPJ B
Condensed Matter and Complex Systems
www.epj.org

Eur. Phys. J. B **64**, 341–347 (2008) DOI: 10.1140/epjb/e2008-00135-8

Life at ultralow interfacial tension: wetting, waves and droplets in demixed colloid-polymer mixtures

H.N.W. Lekkerkerker, V.W.A. de Villeneuve, J.W.J. de Folter, M. Schmidt, Y. Hennequin, D. Bonn, J.O. Indekeu and D.G.A.L. Aarts

EDP SCIENCES
Società Italiana di Fisica
Springer

Eur. Phys. J. B **64**, 341–347 (2008)
DOI: 10.1140/epjb/e2008-00135-8

THE EUROPEAN PHYSICAL JOURNAL B

Life at ultralow interfacial tension: wetting, waves and droplets in demixed colloid-polymer mixtures

H.N.W. Lekkerkerker[1], V.W.A. de Villeneuve[1,a], J.W.J. de Folter[1], M. Schmidt[2], Y. Hennequin[3], D. Bonn[3,4], J.O. Indekeu[5], and D.G.A.L. Aarts[6]

[1] Van't Hoff Laboratory for Physical and Colloid Chemistry, Utrecht University, Padualaan 8, 3584 Utrecht, The Netherlands
[2] H.H. Wills Physics Laboratory, University of Bristol, Tyndall Avenue, Bristol BS8 1TL, UK
[3] Van der Waals-Zeeman Institute, University of Amsterdam, Valckenierstraat 65, 1018XE Amsterdam, The Netherlands
[4] Laboratoire de Physique Statistique, École Normale Supérieure, 24 Rue Lhomond, 75231 Paris Cedex 05, France
[5] Instituut voor Theoretische Fysica, Katholieke Universiteit Leuven 200D, 3001 Leuven, Belgium
[6] Physical and Theoretical Chemistry Laboratory, University of Oxford, South Parks Road, Oxford OX1 3QZ, UK

Received 10 October 2007 / Received in final form 4 February 2008
Published online 2 April 2008 –

Abstract. Mixtures of colloids and polymers display a rich phase behavior, involving colloidal gas (rich in polymer, poor in colloid), colloidal liquid (poor in polymer, rich in colloid) and colloidal crystal phases (poor in polymer, highly ordered colloids). Recently, the colloidal gas-colloidal liquid interface received considerable attention as well. Due to the colloidal length scale the interfacial tension is much lower than in the atomic or molecular analog (nN/m instead of mN/m). This ultra-low interfacial tension has pronounced effects on the kinetics of phase separation, the colloidal gas-liquid profile near a single wall and the thermally induced fluctuations of the interface. The amplitudes of these thermally excited capillary waves are restrained by the interfacial tension and are for that reason of the order of the particle diameter. Therefore, in molecular systems, the capillary waves can only be seen indirectly in scattering experiments. In colloidal systems, however, the wave amplitudes are on a (sub) micrometer scale. This fact enables the direct observation of capillary waves in both real space and real time using confocal scanning laser microscopy. Moreover, the real space technique enables us to demonstrate the strong influence of interface fluctuations on droplet coalescence and droplet break up.

PACS. 67.30.hp – 68.05.Cf Structure: measurements and simulations – 68.37.-d Microscopy of surfaces, interfaces, and thin films – 64.75.Xc Phase separation and segregation in colloidal systems

1 Introduction

At the beginning of the previous century, colloid science and statistical physics with the help of optical microscopy enjoyed an intimate and highly productive relationship. Starting from the seminal work of Einstein [1] on Brownian motion, Perrin [2] with simple, yet brilliant optical microscopy experiments determined quantitatively the sedimentation equilibrium distribution and Brownian motion characteristics of colloidal particles. From these measurements, which are considered to have finally proven the existence of atoms beyond any reasonable doubt, he deduced the first reliable value of Boltzmann's constant, the key quantity underlying statistical physics. For this work Perrin was awarded the 1926 Noble prize in Physics. About 10 years later Smoluchowski [3], inspired by the ultramicroscopy observations of Svedberg [4] on the fluctuating number of colloidal gold particles in a fixed region of space, developed the probability - after-effect method which may be considered as the foundation of the statistical physics of stochastic processes. (For an early review, see Chandrasekhar [5] and for a more recent account, see the book by van Kampen [6])

In 1908 Smoluchowski [7] also developed a statistical physical theory of critical opalescence. The first direct visual observations of critical fluctuations were made by Debye and Jacobsen [8]. They used a phase-contrast microscope to observe the concentration fluctuations in a solution of polystyrene in cyclohexane near its consolute point. While the thermal accuracy of ± 0.02 K achieved by Debye and Jacobsen did not allow a clear separation of the critical fluctuations from the onset of phase separation, the subsequent pictures of critical concentrations fluctuations obtained by Beysens and co-workers [9] with a thermal stabilization of the order of ± 0.2 mK, established the fractal nature of these "clusters", demonstrating the great potential for statistical physics of these direct visual observations. In his 1908 paper Smoluchowski [7] also

[a] e-mail: v.w.a.devilleneuve@uu.nl

predicted that thermal motion inevitably gives rise to statistical fluctuations of the local position of the free interface between two fluids, such as that between a liquid and its vapor. A few years later Mandelstam [10] quantitatively described the interface roughness in terms of thermally excited capillary waves (50 years later Buff et al. [11], apparently unaware of the work of Mandelstam, produced independently, an extended version of the theory). The first direct visual observation of the interface roughness, due to thermally induced capillary waves, was reported in 2004 [12]. This observation was made on the free fluid-fluid interface in a phase separated colloid-polymer suspension with laser scanning confocal microscopy. In these systems the interfacial tension γ can be made ultralow, down to nN/m compared to mN/m for atomic and molecular liquids, leading to a root mean squared amplitude of the height fluctuations on the (sub) micrometer scale.

In this contribution we first review the background and measurement of the ultralow interfacial tension in demixed colloid-polymer suspensions, and describe the measurement and space-time characteristics of thermally excited capillary waves based on direct observations. We then present results which show that thermally excited capillary waves are of crucial importance for the rupture of thin liquid films in droplet coalescence and we show that in systems with ultralow interfacial tension the process of droplet break-up is influenced by thermal height fluctuations on a directly visible scale. We conclude with an outlook of the potential of direct observations of interfacial fluctuations for new developments in statistical physics.

2 Interfacial tension of a phase-separated colloid-polymer mixture

The interfacial tension in atomic and molecular systems scales as [13]

$$\gamma \sim \frac{\varepsilon}{\sigma^2}, \tag{1}$$

where ε is the depth of the minimum in the interaction potential and σ the diameter of the atoms/molecules. For low molecular weight systems $\varepsilon \sim 1$–2×10^{-21} J and $\sigma \sim 0.3$–0.4 nm and hence we find γ in the range of tens of mN/m in agreement with experiment. Equation (1) suggests that to obtain an (ultra) low interfacial one must make ε small and/or σ larger[1]. However, for atomic and molecular systems these quantities are coupled. Larger particles also have a larger ε. On the other hand, in colloidal systems with entropy driven phase transitions, such as the isotropic-nematic phase transition of hard rod dispersions [14], the interfacial tension takes the form [15]:

$$\gamma \sim \frac{kT}{LD} \tag{2}$$

where L is the length and D is the diameter of the rods. With $L \sim 200$ nm and $D \sim 10$ nm, one obtains $\gamma \sim 1$ μN/m, which is indeed observed experimentally [16]. For the I-N interface in a system of platelets one expects

$$\gamma \sim \frac{kT}{D^2} \tag{3}$$

with D the diameter of the platelets one expects interfacial tensions as low as a few nN/m, which was confirmed experimentally as well [17].

In the above mentioned systems the phase transitions are between an isotropic and an (orientationally) ordered phase. A colloidal system that shows an entropy driven phase transition, which closely resembles the liquid-gas transition in atomic and molecular systems, is a mixture of colloids with non-adsorbing polymers. The addition of non-adsorbing polymers to a colloidal dispersion can induce a phase separation due to the depletion interaction between the colloids [18–20]. The depletion interaction is based on the fact that there is a region around the colloidal particles, the depletion zone, from which the polymers are almost entirely excluded. When colloidal particles approach each other sufficiently close for the depletion zones to overlap there is an imbalance due to the osmotic pressure exerted by the polymers. This imbalance induces an effective attraction between the colloidal particles (see Fig. 1).

The range of the associated depletion potential depends on the size of the polymer; its depth is proportional to the osmotic pressure which in turn is a function of the concentration of the polymers. Provided the attraction is sufficiently strong ($\sim kT$) and the polymer to colloid size is sufficiently large (>0.3), the colloid-polymer suspension phase separates into two different fluid phases: one colloid-rich ("liquid") and one polymer-rich ("gas") (see Fig. 2).

The interfacial tension between these two phases was measured for a system consisting of a mixture of organophilic silica colloids with a diameter $\sigma = 26$ nm and polydimethyl siloxane (PDMS) with a molecular weight of 91.7 kg/mol and a diameter of 28 nm in cyclohexane. Two different techniques were used: the spinning drop method [21,22] and from the interfacial profile near a single wall [23]. The elongation of a spinning droplet due to the centrifugal pressure difference ($\sim \Delta\rho\omega^2 R^2$)), is balanced by the Laplace pressure difference between the two phases ($\sim \gamma/R$), see Figure 3. Here, $\Delta\rho$ is the density difference, ω rotational speed in rad/s and γ is the interfacial tension. From the measurement of the length L and the radius R of the droplet, the interfacial tension γ can be calculated, using the expression derived by Princen et al. [24]

$$\gamma = \frac{\omega^2 a^3 \Delta\rho}{2\alpha} \tag{4}$$

here a is the radius of curvature of the top of the drop and α is a dimensionless number, both of which are determined by L and R. For the system mentioned above, values for γ in the range 3–4.5 μN/m were obtained [21,22] in good

[1] We are momentarily not concerned with the alternative possibility of moving closer to a bulk critical point, which is another way to lower the interfacial tension, but will return to it later in Section 3.

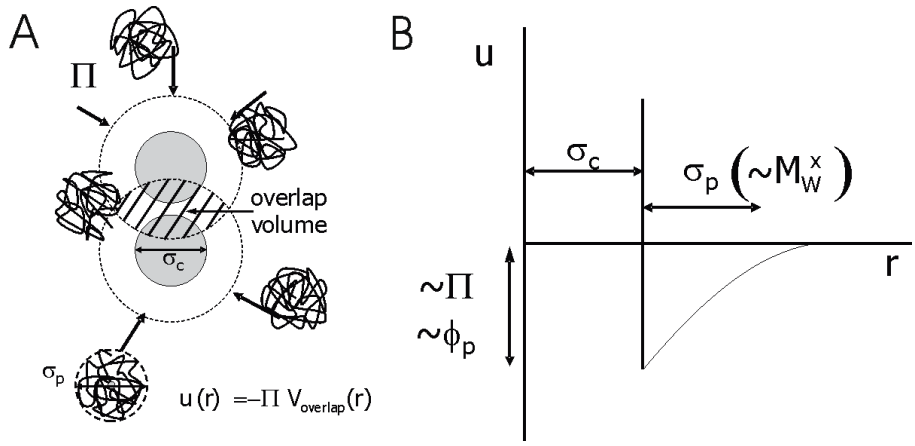

Fig. 1. (A) Two Colloids with diameter σ_c in a sea of polymers with diameter σ_p exerting an osmotic pressure Π. No polymer is present in the depletion zones around the colloids, leading to an effective interaction proportional to the osmotic pressure and the overlap volume of the depletion zones. (B) Schematic representation of the interaction potential between two colloids in a sea of polymers. In a addition to the hard sphere repulsion, there is a short range attraction with a width proportional to σ_p and a depth proportional to the osmotic pressure.

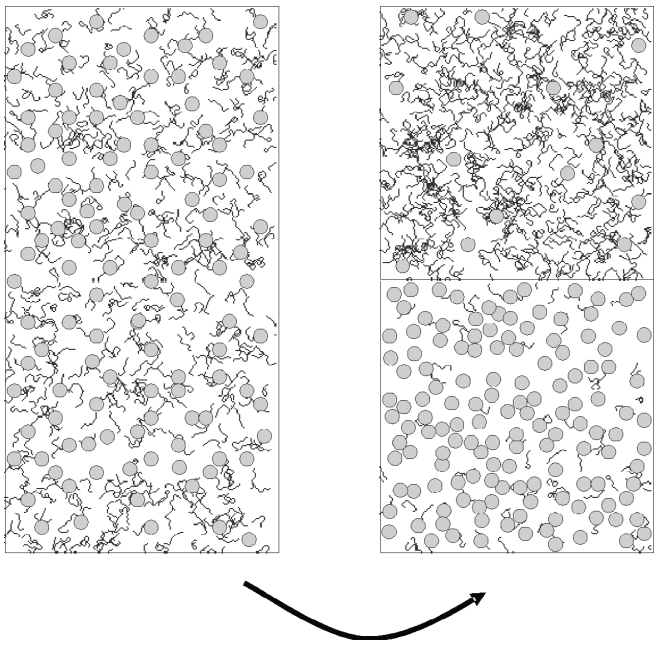

Fig. 2. Schematic representation of the demixing of an initially homogenous colloid-polymer suspension in a coexisting colloid-rich (colloidal liquid) and colloid poor (colloidal gas) phase.

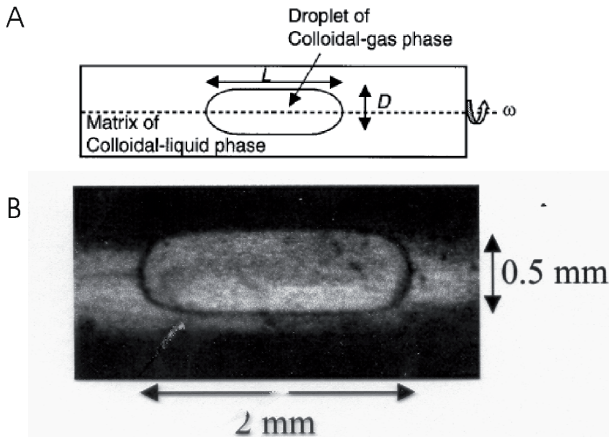

Fig. 3. (A) Schematic representation of a spinning drop tube filled with a droplet of colloidal gas phase surrounded by a matrix of colloidal liquid phase. The system is rotating around its axis with a rotational speed ω. (B) Photograph of a rotating spinning drop tube with a droplet of the low density colloidal gas phase immersed in the high density colloidal liquid phase.

agreement with the scaling relation

$$\gamma \sim \frac{kT}{\sigma^2}. \tag{5}$$

The interfacial profile at a single wall is determined by the balance between hydrostatic pressure ($\Delta\rho g z$) and Laplace pressure (γ/R, R local radius of curvature of the interface). This yields the equation for the profile close to a planar surface:

$$y = L_C \Bigg\{ \cosh^{-1}\frac{2L_C}{z} - \cosh^{-1}\frac{2L_C}{h} + \left(4 - \frac{h^2}{L_C^2}\right)^{\frac{1}{2}} - \left(4 - \frac{z^2}{L_C^2}\right)^{\frac{1}{2}} \Bigg\} \tag{6}$$

where the capillary length is given by $L_C = \sqrt{\gamma/\Delta\rho g}$ While in principle simpler than the spinning drop method, the determination of the profile requires careful optical microscopy measurements. Aarts et al. [23] succeeded in performing such measurements (Fig. 4) and obtained results in good agreement with the spinning drop measurement.

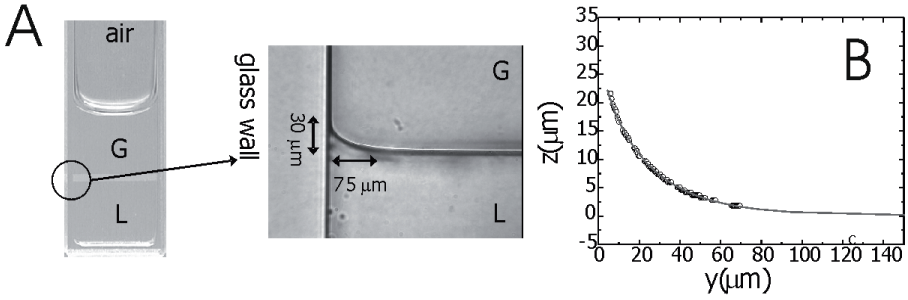

Fig. 4. (A) photograph of a demixed colloid-polymer mixture and a blow-up of the encircled region by transmission light microscopy. L and G indicate the colloidal liquid and gas phases. (B) Measurement of the interfacial profile from light microscopy.

3 Space-time characteristics of thermally excited capillary waves

From the theory of Mandelstam [10] it follows that the mean squared amplitude $\langle h^2 \rangle$ of thermally excited capillary waves is proportional to $\frac{k_B T}{\gamma}$. Combined with the scaling relation (5) for the interfacial tension, this leads to

$$\langle h^2 \rangle \sim \frac{k_B T}{\gamma} \sim \sigma^2. \tag{7}$$

In order to observe the thermally excited capillary waves with optical microscopy, the height fluctuations have to be at least of the order of 0.1 μm. We therefore used a system of colloidal particles with a diameter of 124 nm (fluorescent PMMA particles) in decalin, to which we added polystyrene with a molecular weight of 2×10^6 kg/mol (diameter 86 nm). In Fig. 5 we present confocal microscopy images of the interface approaching the critical point. Clearly, the interfacial fluctuations become larger (reflecting the decrease of γ) and the two coexisting phases become more and more similar.

In order to obtain quantitative information we determine the space-time characteristics of the thermally excited capillary waves through height-height correlations at two different space points at equal times and at two different times at equal space points (see Fig. 6).

The spatial correlation

$$g_h(x,t) = \left\langle \left[h(x',t') - \bar{h}(t')\right] \times \left[h(x'+x,t'+t) - \bar{h}(t'+t)\right] \right\rangle \tag{8}$$

is obtained by Fourier transforming results of Mandelstam [10] for the amplitudes of the thermally excited capillary waves. This yields (see e.g. [25])

$$g_h(x) = \frac{k_B T}{2\pi\gamma} K_0\left(\frac{x}{L_c}\right), \tag{9}$$

where K_0 is the modified Bessel function of the second kind. Note that this function diverges for $x \to 0$. The reason being that in the Fourier transformation leading to equation (9), no cut off for the large k values has been used, while physically $k_{\max} \sim \frac{2\pi}{\sigma}$. In Figure 7 we show experimental results for $g_h(x)$ and their fit to the theoretical expression. From it we obtain $\gamma = 19$ nN m^{-1} and

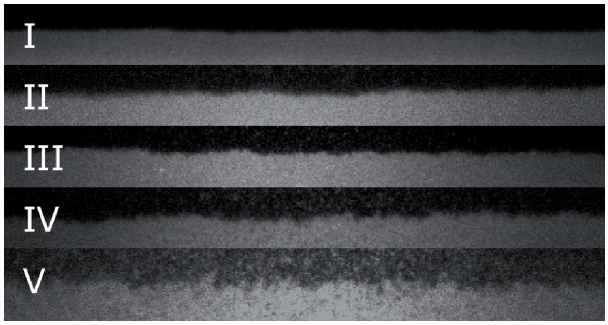

Fig. 5. Confocal microscopy images of 5 statepoints with different colloid polymer concentrations of the same system approaching the binodal. Colloid (ϕ_c) and polymer (ϕ_p) volume fractions: I. $\phi_c = 0.223$, $\phi_p = 0.797$; II. $\phi_c = 0.213$, $\phi_p = 0.761$; III. $\phi_c = 0.207$, $\phi_p = 0.739$; IV. $\phi_c = 0.198$, $\phi_p = 0.708$; V. $\phi_c = 0.195$, $\phi_p = 0.695$. The polymer volume fractions are calculated from spheres with a diameter of twice the radius of gyration.

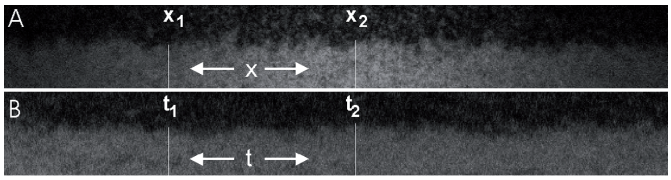

Fig. 6. Characterizing capillary waves by confocal microscopy. (A) The correlation between heights at two different positions on the interface at a fixed time. (B) The correlation between heights at two different times at a fixed interfacial position.

$L_c = 8.4$ μm. The fit is good, but a full understanding of the small deviations might require extended theory such as in [26,27].

Due to the ultralow value of γ the capillary waves in the phase separated colloid-polymer mixture are overdamped with a damping factor [28,29]

$$\Gamma_k = \frac{[kL_c + 1/kL_c]}{2\tau_{cap}} \tag{10}$$

where the capillary time is given by the expression:

$$\tau_{cap} = \frac{(\eta_{gas} + \eta_{liq})L_c}{\gamma}, \tag{11}$$

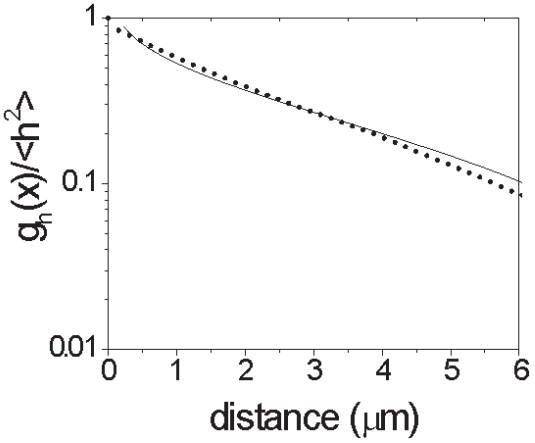

Fig. 7. Spatial correlation function for statepoint IV (see Fig. 5 for details).

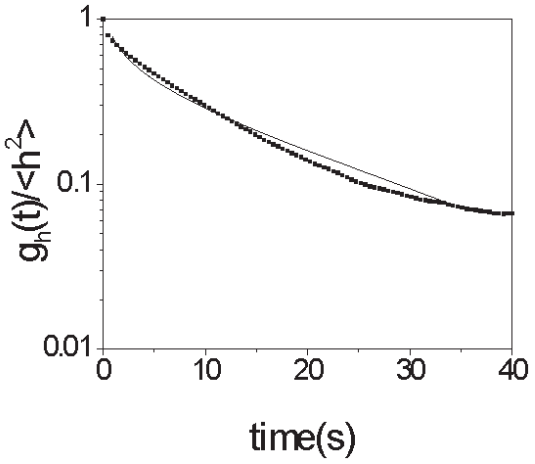

Fig. 8. Time correlation function for statepoint IV (see Fig 5 for details).

which for colloidal systems is raised by $\sim 10^5$ to 1–100 s. Besides the length scales, this timescale is a key element for clearing the path towards microscopy measurements of capillary waves.

Again Fourier transforming, taking into account the damping factor (10), one obtains

$$g_h(t) = \langle h(x,t')h(x,t'+t)\rangle = \frac{k_B T}{2\pi\gamma}\int_0^\infty d\,(kL_c)\,(kL_c) \times \frac{\exp\left(-\left(kL_c + (kL_c)^{-1}\right)t/(2\tau_{cap})\right)}{1+(kL_c)^2}. \quad (12)$$

In Figure 8 we show experimental results for $g_h(t)$ (it is difficult to obtain statistically accurate values for large times) and their fit to theoretical expression (12). From the fit we obtain $\gamma = 25$ nN m^{-1} and $\tau_{cap} = 22$ s. From the interfacial tensions, capillary length and capillary time obtained from the height correlation functions we obtain a value of 60–80 mPa s for the combined viscosities of the phases, which is reasonable.

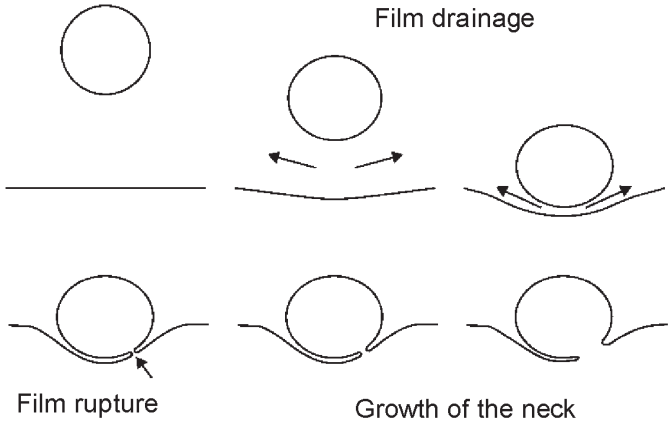

Fig. 9. Schematic drawing of the consecutive stages of droplet coalescence.

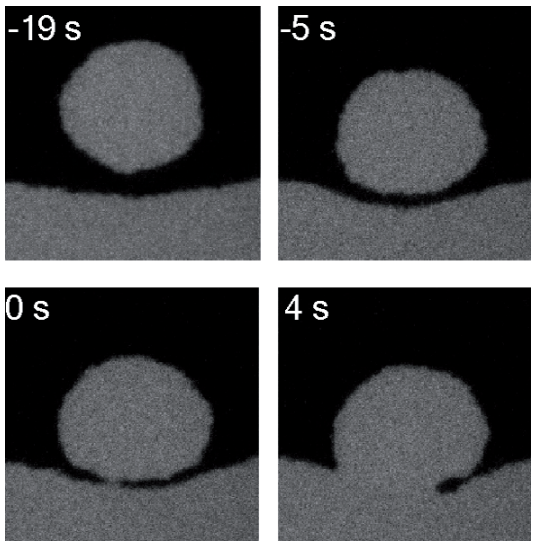

Fig. 10. Confocal microscopy images of the consecutive stages of droplet coalescence, showing film drainage, film rupter and growth of the neck.

4 Droplet coalescence

The process of droplet coalescence is frequently observed in every day life. Whenever two liquid drops or a liquid drop and its bulk liquid come into contact, they may coalesce. The coalescence reduces the total interfacial area and is driven by interfacial tension. The phenomenon has been studied since the 19th century [30]. One may distinguish three stages in droplet coalescence: (i) film drainage, (ii) film rupture and (iii) growth of the neck. These consecutive stages are schematically illustrated in Figure 9. The film drainage [31] and the growth of the neck [32] have been studied extensively and the film rupture has been studied in relation in connection with film drainage [33,34]. Using a phase separated colloid polymer mixture we obtained for the first time [12] direct visual evidence for the crucial role of thermally excited capillary waves in the rupture event (see Fig. 10). Decreasing the surface tension by a factor of 10^5 opens the way to

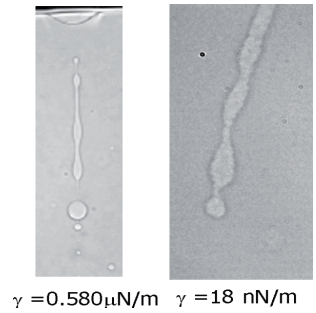

Fig. 11. Droplet snap-off at different interfacial tensions. In the left figure thermal noise does not visibly affect the break-up of the thread, while in the right figure the thermal noise does affect the shape of the break-up event.

a more complete understanding of the hydrodynamics involved [35].

The kinetics of the coalescence event is determined by the competition between (slow) drainage of the film and the waiting time for a large fluctuation to rupture the film. While we have been able to determine waiting times as a function of state point [36], no complete theory for the kinetics of droplet coalescence incorporating interfacial fluctuations is available.

5 Break-up of liquid jets

Jet break-up [37] is closely related to the Rayleigh-Tomotika [38,39] mechanism of the instability of a liquid column. This mechanism of break up involves flow from regions of the liquid column with smaller radii (necks where the Laplace pressure is larger) to bulges where the pressure is lower, until pinch-off occurs. Out of all unstable disturbances, the fastest growing one has a wavelength of about ten times the column's radius. Using molecular dynamics simulations, Moseler and Landman [40] discovered that in the break up of nanojets thermal fluctuations play a decisive role. They were able to account for their MD results by adding to the Navier Stokes equations a fluctuating stress first introduced by Landau and Lifshitz [41]. It is easy to estimate [42] that this fluctuating stress becomes dominant over capillary forces at length scales of the order of the thermal length $L_T = \sqrt{k_B T/\gamma}$. Therefore one expects that these fluctuating stresses become important on the nanoscale for atomic and molecular liquids as was indeed observed in the computer simulations by Moseler and Landman [40]. At the same time one expects them to become visible in a real experiment for ultralow interfacial tension systems as is indeed the case [42], see Figure 11.

6 Conclusions and outlook

In this contribution we have shown that thermally excited capillary waves at the fluid-fluid interface in a phase separated colloid-polymer suspension can be directly observed with confocal microscopy. The space-time characteristics which can be determined from these confocal microscopy measurements are on the whole well described by the standard capillary wave model [10,11]. However, it is certainly worthwhile to see whether the data provide indications for phenomenological extensions of the capillary wave model [26,27], for example with an elastic energy. Such evidence may show up more clearly in tilt angle distributions, which can also be obtained from the confocal images [43]. These tilt angle distributions sample the second moment of the capillary wave spectrum [27] and are therefore more sensitive to the bending elastic term. We have also shown that the thermally excited capillary waves are of crucial importance for droplet coalescence and droplet break-up. For droplet coalescence, the competition between film drainage and waiting times for large fluctuations determines the stochastics of droplet coalescence. This problem still deserves further attention. For droplet break-up we see that (Fig. 11) there seems to be a fairly sharp transition from a *smooth* pattern to a more *corrugated* pattern on decreasing the interfacial tension. This requires further analysis.

So far we have considered thermally excited capillary waves at a free interface. We have also observed capillary waves on wetting layers in colloid-polymer mixtures [44]. From these measurements we obtained evidence of an interfacial roughness $\xi_\perp^2$ proportional to the wetting layer thickness. Such a dependence has indeed been predicted for short range forces in $d = 3$ [45,46]. No simulations or experiments have reported this yet.

In conclusion the direct observation of thermally excited capillary waves, both at the free fluid-fluid interface as well as on wetting layers, opens new possibilities and challenges in statistical physics.

The work of V.W.A.d.V. is part of the research program of the 'Stichting voor Fundamenteel Onderzoek der Materie (FOM)', which is financially supported by the 'Nederlandse Organisatie voor Wetenschappelijk Onderzoek (NWO)'. Support of V.W.A.d.V. by the DFG through the SFB TR6 is acknowledged. J.O.I. thanks the FWO-Vlaanderen for support through Project G.0483.04.

References

1. A. Einstein, Ann. D. Physik **17**, 549 (1905)
2. J. Perrin, Ann. Chim. Phys. **18**, 5 (1909)
3. M. Smoluchowski, Wien. Ber. **123**, 2381 (1914); M. Smoluchowski, Wien. Ber. **124**, 339 (1915)
4. T. Svedberg, Z. Phys. Chem. **77**, 147 (1911)
5. S. Chandrasekhar, Rev. Mod. Phys. **15**, 1 (1943)
6. N.G. van Kampen, *Stochastic Processes in Physics and Chemistry* (North-Holland, Amsterdam, 1981)
7. M. Smoluchowski, Ann. D. Physik **25**, 205 (1908)
8. P. Debye, R.T. Jacobsen, J. Chem. Phys. **48**, 203 (1968)

9. D. Beysens, P. Guenon, F. Perrot, J. Phys.: Condens. Matter **2**, SA127 (1991)
10. L. Mandelstam, Ann. D. Physik **41**, 609 (1914)
11. F.P. Buff, R.A. Lovett, F.H. Stillinger, Phys. Rev. Lett. **15**, 621 (1965)
12. D.G.A.L. Aarts, M. Schmidt, H.N.W. Lekkerkerker, Science **304**, 847 (2004)
13. J.S. Rowlinson, B. Widom, *Molecular Theory of Capillarity* (Clarendon Press, Oxford, 1982)
14. L. Onsager, An.. N.Y. Acad. Sci. **51**, 627 (1949)
15. K. Shundyak, R. Van Roij, J. Phys.: Condens. Matter **13**, 4789 (2001)
16. W. Chen, D.G. Gray, Langmuir **18**, 633 (2002)
17. D. van der Beek, H. Reich, P. van der Schoot, M. Dijkstra, T. Schilling, R. Vink, M. Schmidt, R. van Roij, H.N.W. Lekkerkerker, Phys. Rev. Lett. **97**, 087801 (2006)
18. S. Asakura, F. Oosawa, J. Chem. Phys. **22**, 1255 (1954)
19. A. Vrij, Pure Appl. Chem. **48**, 471 (1976)
20. H.N.W. Lekkerkerker, W.C. Poon, P.N. Pusey, A. Stroobants, P.B. Warren, Europhys. Lett. **20**, 559 (1992)
21. G.A. Vliegenthart, H.N.W. Lekkerkerker, Progr. Colloid Polym. Sci. **105**, 27 (1997)
22. E.H. de Hoog, H.N.W. Lekkerkerker, J. Phys. Chem. B **103**, 5274 (1999)
23. D.G.A.L. Aarts, J.H. van der Wiel, H.N.W. Lekkerkerker, J. Phys.: Condens. Matt. **15**, s245 (2003)
24. H.M. Princen, I.Y.Z. Zia, S.G. Mason, J. Colloid Interface Sci. **23**, 99 (1967)
25. M. Tolan, O.H. Seeck, J.P Schlomka, W. Press, J. Wang, S.K. Sinha, Z. Li, M.H. Rafailovich, J. Sokolov, Phys. Rev. Lett. **81**, 2731 (1998)
26. J. Meunier, J. Physique. Lett. **46**, L 1005 (1985)
27. K. Mecke, S. Dietrich, J. Chem. Phys. **123**, 204723 (2005)
28. J. Meunier, in *Liquids at Interfaces*, edited by J. Charvolin, J.F. Joanny, J. Zinn-Justin (North-Holland, New York, 1988), p. 327
29. U.S. Jeng, L. Esibov, L. Crow, A. Steyerl, J. Phys.: Condens. Matter **10**, 4955 (1998)
30. J. Thomson, H. Newall, Proc. R. Soc. London **39**, 417 (1885)
31. A.F. Jones, S.D.R. Wilson, J. Fluid Mech. **87**, 263 (1978)
32. J. Eggers, J.R. Litster, H.A. Stone, J. Fluid Mech. **401**, 293 (1999)
33. G.V. Jeffreys, J.L Hawksley, J. Appl. Chem. **12**, 329 (1962)
34. A.H. Brown, C. Hanson, Nature **214**, 76 (1967)
35. D.G.A.L. Aarts, H.N.W. Lekkerkerker, H. Guo, G. Wegdam, D. Bonn, Phys. Rev. Lett. **95**, 164503 (2005)
36. D.G.A.L. Aarts, H.N.W. Lekkerkerker, J. Fluid Mech., to be published
37. J. Eggers, Rev. Mat. Phys. **69**, 865 (1997)
38. J.W.S. Rayleigh, Proc. R. Soc. London **10**, 4 (1879)
39. S. Tomotika, Proc. R. Soc. London A **150**, 322 (1935)
40. M. Moseler, U. Landman, Science **289**, 1165 (2000)
41. L. D. Landau, E.M. Lifshitz, J. Exp. Theor. Phys. (USSR) **32**, 618 (1957)
42. Y. Hennequin, D.G.A.L Aarts, J.H. van der Wiel, G. Wegdam, J. Eggers, H.N.W. Lekkerkerker, D. Bonn, Phys. Rev. Lett. **97**, 244502 (2006)
43. D.G.A.L Aarts, M. Schmidt, H.N.W. Lekkerkerker, K.R. Mecke, Adv. In Solid State Phys. **45**, 15 (2005)
44. Y. Hennequin, D.G.A.L Aarts, J.O. Indekeu, H.N.W. Lekkerkerker, D. Bonn, Phys. Rev. Lett., submitted for publication
45. D.S. Fisher, D.A. Huse, Phys. Rev. B **32**, 247 (1985)
46. R. Lipowsky, M.E. Fisher, Phys. Rev. B **36**, 2126 (1987)